

Study of molecular mechanisms of learning and memory impairment in neonatal rats post intrauterine distress via the pathway of Tau protein hyperphosphorylation

X.-S. WANG, H. HUANG

Department of Obstetrics and Gynecology, Chongqing Traditional Chinese Medicine Hospital, Chongqing, China

Abstract. – **OBJECTIVE:** To explore the reversal of the excitatory amino acid receptor antagonists against the impairment of learning-memory and the hyperphosphorylation of protein Tau induced by fetal intrauterine distress in neonatal rats.

MATERIALS AND METHODS: The analysis of variance of factorial design set up two intervention factors, fetal intrauterine distress (two levels: no fetal intrauterine distress and a course of fetal intrauterine distress) and the excitatory amino acid receptor antagonists (three levels: Saline; NMDA receptor antagonist MK-801; astragalosides). Forty-eight pregnant rats were randomly divided into six experimental groups ($n=8$, in each group). After the end of the fetal intrauterine distress, the pregnant rats continued until the birth of newborn rats. When the neonatal rats grow to 12W, the Morris water maze test started in order to evaluate learning-memory. The hippocampus was removed from newborn rats within 1 day after the Morris water maze test finished. The content of glutamate in the hippocampus of rats was detected by high performance liquid chromatography. Besides, the content of protein Tau including Tau5 (total protein Tau), p-PHF1^{Ser396/404}, p-AT8^{Ser199/202}, p-12E8^{Ser262} in the hippocampus of rats, was examined with the method of immunohistochemistry (IHC) staining (SP).

RESULTS: Fetal intrauterine distress and the glutamate ionic receptor blockers could induce the impairment of learning-memory in neonatal rats, extending the evasive latency time and shorten the space exploration time. Both influences present subtract effect. Fetal intrauterine distress could significantly up-regulate the content of glutamate in the hippocampus of neonatal rats, which was not affected by the glutamate ionic receptor blockers. Fetal intrauterine distress and the glutamate ionic receptor blockers did not affect the total protein Tau in the hippocampus of rats. Moreover, fetal intrauterine distress could increase the hyperphosphorylation of protein Tau in the hippocampus of neonatal rats, which were reduced by the glutamate ionic

receptor blockers. Both influences presented subtract effect.

CONCLUSIONS: We showed that fetal intrauterine distress upregulates the content of glutamate in the hippocampus of neonatal rats, up-regulating the hyperphosphorylation of protein Tau and inducing the impairment of learning-memory in neonatal rats.

Key Words

Tau protein, DNQX, Excitatory toxicity, Glutamic acid, Intrauterine distress.

Introduction

Fetal intrauterine distress (FIUD) refers to the acidosis of the fetus in the uterus due to ischemia and hypoxia and the emergence of a series of fetal dying syndrome, whose incentives are oxygen transport and exchange dysfunction. Fetal distress can lead to neonatal asphyxia, which can cause some degree of neonatal neuronal damage. Fetal intrauterine distress is one of the most important causes of hypoxic-ischemic encephalopathy (HIE), which seriously affects the cognitive development of children. The concentration of glutamate in the hippocampus increases due to hypoxia and oxidative stress caused by FIUD, then inducing neuronal excitotoxicity, eventually leading to neonatal cognitive impairment. DNQX (6,7-dinitroquinoxaline-2,3-dione) can inhibit neuronal synthesis and release glutamate and NMDA receptor antagonists can prevent it by blocking excitotoxicity. Whether DNQX is a natural glutamate receptor antagonist, can it prevent fetal distress induced ischemia and hypoxia stress process? Therefore, we aimed at exploring the molecular mechanisms of learning and memory impairment in neonatal rats post intrauterine

distress *via* the pathway of Tau protein hyperphosphorylation.

Materials and Methods

Major Reagents and Instruments

Pure 5-methyldipropylcyclohexene imine maleic acid (MK-801, NMDA Receptor Antagonist Sigma-Aldrich, St. Louis, MO, USA); rabbit monoclonal antibody against p-AT8Ser202 (Gene Tex, San Antonio, TX, USA); mouse monoclonal antibody against human GSK-3 β 1H8 (Santa Cruz Biotechnology, Santa Cruz, CA, USA); pure 5-methyldihydropropane gumene maleimide (MK-801, which is NMDA receptor antagonist; Sigma-Aldrich, St. Louis, MO, USA); mouse anti-bovine taurine 5 monoclonal antibody (Millipore, Billerica, MA, USA); rabbit anti-bovine p-PHF1Ser396/404 monoclonal antibody (Abcam, Cambridge, MA, USA); rabbit anti-human p-AT8Ser199/202 polyclonal antibody (Invitrogen, Carlsbad, CA, USA); rabbit anti-human p-12E8Ser262 polyclonal antibody (Life Span Biosciences, Seattle, WA, USA); pure L-glutamic acid (L-Glutamic acid, Sigma-Aldrich, St. Louis, MO, USA); HPLC chromatography system (Waters, Polk, FL, USA); protein electrophoresis system (Bio-Rad, Hercules, CA, USA); golden disk multimedia image processing system (Chengdu Gold Disk Electronic Technology Co., Ltd. Chengdu, China); SM600 automatic microplate reader (Shanghai Wing Chong Medical Devices Co., Ltd., Shanghai, China).

Experimental Animals

24-week-old Sprague-Dawley rats (SPF) with a weight of 275-300 g were obtained from Animal center of Inner Mongolia Medical University (No. 012). All rats were fed with standard rat feeds, free to drink water. They received a daily touch of habituation to a laboratory environment. This study was approved by the Animal Ethics Committee of Chongqing Traditional Chinese Medicine Hospital Animal Center.

Experimental Methods

Principles of Animal Experiment

The experiment was conducted according to the American Medical Research Association's "Principles of Experimental Animal Processing" and the American Society for Science and National Institutes of Health "Guidelines for the Use and Handling of Laboratory Animals". The blind principle was in double, and rats were fed in a single cage.

Establishment of Animal Mode

The well-developed Sprague-Dawley (SD) rats, which were selected, weighted about 300 g and could move freely without significant deformity. The rats were fed in a cage according to the ratio of female:male=1:2. After keeping the cage, the researchers needed to use a cotton swab every day to wipe the female vagina using the vaginal semen smear test; if it was positive, the day would be recorded as the first day of pregnancy, and for high nutrition of the feed for feeding.

After that, researchers should touch the female rat's abdomen daily and check whether the abdomen had a swollen pregnancy continuously. If there was no uterine bulging phenomenon for ten days in a row, it could be considered a failure for the conception process of the female. 18-day-old pregnancy SD rats were used to make animal model, in accordance with the operation steps of the references¹⁻⁴: 1) Animals were weighed with a balance. 2) 1 mL/100 g 3.5% hydrated chlorhexidine was injected in the tail vein. 3) Animals were fixed with supine on the mouse board. 4) 5% iodophor disinfected abdominal skin twice. 5) Pregnancy uterus was exposed via the lower abdomen median incision under aseptic conditions, so as to observe live births within the intrauterine bilaterally. 6) Small artery hemostatic forceps were placed in the medial at the upper and lower ends of unilateral uterus, respectively. The occurrence of fetal rats intrauterine distress was due to uterine and placental circulatory disorder, reperfusion would be achieved after the removal of the artery clamp in the time required to achieve ischemia, and then fetal rat should be put back to the uterus and close the abdominal cavity by layer. SD rats were returned to the cage for feeding until full-term pregnancy and re-anesthesia laparotomy; newborns were delivered via cesarean section. Note: uterine arteries were clipped with a special micro non-invasive vascular clamp. 7) After cesarean section, newborn rats were routinely kept in a warm box, and then stroked and weighed daily, fed for 4 weeks until the swimming ability test; those who cannot swim or move normally should be screened out.

Experimental Animal Grouping

Factorial design was done for each rat with two management factors, namely FIUD treatment and GluR antagonist [including injection of saline, NMDA receptor (N-methyl-D-aspartic acid receptor) antagonist MK-801, AMPA receptor (α -amino-3-hydroxy-5-methylisoxazole-4- propi-

onic acid) antagonist DNQX (6,7-dinitroquinoxaline-2,3-dione)]. Based on this, rats were divided into 6 groups with 8 rats in each group.

Detection of the Spatial Cognitive Ability of Experimental Rats with Morris Water Maze Video Analysis System⁵

After all the fetal distress treatments of the mother who delivered newborns, and when the newborns grew to 12W, Morris water maze test process began. Morris water maze forced rats to swim so that they learned to find an experimental platform submerged in water. Morris water maze played roles in evaluating the spatial learning and memory abilities of the tested animals in the spatial direction. Morris water maze system contains Morris water maze main part, video capture of the memory card, and CCD acquisition data of the camera. In Morris water maze, the water depth was 42 cm, the temperature of the water pool was about 23-25°C, and a platform was placed 2 cm below the surface of the water with a diameter of 8 cm and a height of 40 cm. At the same time, Morris water maze had four quadrants, and turns were used in accordance with the experiment.

Materials

The hippocampus of rats was removed within 24 h after the end of the Morris water maze test. The specific procedures are as follows: the experimental rats were fasted for 8 h before exercise, drunk freely, and received intravenous injection of 1.5 g/kg 20% animal anesthetic. Urea ethane was applied for anesthesia, and the experimental rats were sacrificed at the same time using a homologous rat-headed guillotine, followed by craniotomy. Finally the whole brain of the experimental rats was removed. After removal of diethyl pyrocarbonate (DEPC) above the ice and the full absorption of brain tissue blood, the rat bilateral hippocampi were isolated. The left hippocampus was weighed and added with 1 mL of methanol-water and homogenized at low temperature, and then a portion of the homogenate was taken out at 4°C and centrifuged at 12,000 μg for 15 min. Subsequently, the supernatant was removed, and the filter treatment was performed. The hippocampus tissues were placed at -80°C refrigerator for preservation, and the specific content of glutamic acid was measured. The hippocampus tissues on the right side were placed in

a 10% paraformaldehyde at 4°C for three days and then subjected to a dehydration treatment. Next, the tissues were embedded in paraffin, and subjected to a slice treatment (thickness of about 1 μm). The immunohistochemistry was performed by immunohistochemistry-streptavidin-peroxidase (IHC-SP) and chromatin.

Detection of Glu in the Hippocampus with High Performance Liquid Chromatography (HPLC)⁶

Well-prepared SD rat hippocampi received homogenate with supernatant. 18-ODS column temperature was 35°C. The mobile phase was filtered through a 0.45 μm microporous membrane and degassed by ultrasounds. The flow rate was 1.0 $\text{mL}\cdot\text{min}^{-1}$, the excitation wavelength was 250 nm, the emission wavelength was 410 nm, and the Glu peak area was quantified. Amino acid standard solution was prepared by Glu standard dubbed, 100 $\mu\text{mol}\cdot\text{L}^{-1}$ standard solution, and pre-test dilution. Derivation and analysis: 100 μL standard solution or tissue sample solution were taken using an EP tube, and 100 μL derivatization reagents were added for reaction for 2 min after the injection of 20 μL reagents. The Glu standard curve was established with Glu standard solution at a concentration of 0.15 mg/L, 0.30 mg/L, 0.735 mg/L, 1.47 mg/L, 2.94 mg/L, 3.675 mg/L, 5.88 mg/L. After derivatization treatment, the external standard method was adopted for quantitative analysis. Glu content in the hippocampus was determined by thawing of the hippocampal homogenate supernatant, addition of frozen formic acid (1 $\text{mol}\cdot\text{L}^{-1}$, 2 mL), and homogenizing under ice bath. The homogenate was centrifuged at 4°C and 7000 $\text{r}\cdot\text{min}^{-1}$ for 30 min. After that, the supernatant was taken at -20°C, and 1 mL brain tissue homogenate supernatants was added with 0.75 mL 4% sodium bicarbonate solution for centrifugation at 4°C and 3000 $\text{r}\cdot\text{min}^{-1}$ for 5 min. Subsequently, the supernatant was taken out and placed into 0.45 μm filter for sub-packaging. 24 μL packing solution with 960 μL sodium tetraborate buffer (pH 9.18) were added at 20°C for 3 min after the injection, followed by gradient washing. Finally, the Glu content was determined.

Detection of Tau Protein Expression in Hippocampus in Rats by IHC-SP.⁷ ***Tau Protein 5, p-PHF1^{Ser396/404}, p-AT8^{Ser199/202}, p-12E8^{Ser262}***

Firstly, samples were pretreated. They underwent conventional dewaxing and hydrated with

ethanol, followed by rinsing with distilled water. Then, the tissues were immersed in 0.01 mol/L phosphate-buffered saline (PBS) solution for 5 min, and dipped with 3% H₂O₂ for 15 min. After that, 0.01 mol/L citric acid solution was added for reaction for 20 min, and then the tissues were cooled at room temperature for 20 min, followed by incubation using 10% sheep serum for 15 min. Secondly, antibodies were added for incubation. 50 μ L corresponding antibodies (mouse anti-bovine tartin 5 monoclonal antibody, rabbit anti-bovine p-PHF1Ser396/404 monoclonal antibody, P-AT8Ser199/202 polyclonal antibody, and rabbit anti-human p-12E8Ser262 polyclonal antibody) (diluted at 1:400) were added for incubation at 37°C for 120 min. 50 μ L of IgG working solution were added for incubation at 37°C for 25 min. Subsequently, 50 μ L streptavidin were added for incubation at 37°C for 25 min. Thirdly, samples were stained. DAB solution was added for 5 min of color development, followed by rinsing with 0.01 mol/L PBS. Fourthly, pictures were taken after color development, and the analysis was performed (with 0.01 mol/L PBS solution as the negative control).

Statistical Analysis

Measurement data were expressed by mean \pm standard deviation (SD) ($\bar{x} \pm s$). SPSS 20.0 statistical software package (IBM, Armonk, NY, USA) was used to test the variance of the sam-

ples. The test results showed that the variance was uniform. In this study, the factorial variance analysis method was used to analyze the interaction effect and main effect of each factor. Comparison between groups was conducted using one-way ANOVA (Analysis of Variance) followed by Least Significant Difference (LSD). $p < 0.05$ or $p < 0.01$ represented that the difference was statistically significant.

Results

Comparisons of Learning and Memory Scores with Morris Water Maze

Fetal intrauterine distress-induced ischemia and hypoxia ($F=20.077$, $p=0.000$) and glutamate receptor antagonists ($F=9.301$, $p=0.000$) might cause learning and memory dysfunction in rats, so as to avoid prolonged latency. Besides, the space exploration time was shortened, but the effect of the two intervention factors was attenuated (escape latency: $F=112.365$, $p=0.000$, glutamate receptor antagonist: $F=22.184$, $p=0.000$, and space exploration time: $F=110.565$, $p=0.000$). This indicates that fetal distress-induced ischemia and hypoxia and glutamate receptor antagonists are superimposed, and the degrees of learning and memory impairments are significantly reduced (Tables I, II).

Table I. Comparison of learning and memory scores of Morris water maze test: EL(s) ($\bar{x} \pm s$, $n=8$).

Groups	Saline	MK-801	CNOX	Sum	F	p
Blank	36.92 \pm 5.23	61.07 \pm 6.20	60.57 \pm 7.36	52.85 \pm 12.99	38.030	0.000
FIUD	90.99 \pm 11.72	49.02 \pm 6.31	46.86 \pm 4.64	62.29 \pm 22.15	74.617	0.000
Sum	63.95 \pm 29.25	55.00 \pm 8.66	53.72 \pm 9.24	57.57 \pm 18.58	9.319*	0.000*
F	147.713	14.815	19.833	20.077*	($F=112.365$,	
p	0.000	0.002	0.001	0.000*	$p=0.000$) [#]	

*The F -value and the p -value of the main effect; [#]The F and p -values of the interaction effect.

Table II. Comparison of learning and memory scores of Morris water maze test: SET(s) ($\bar{x} \pm s$, $n=80$).

Groups	Saline	MK-801	CNOX	Sum	F	p
Blank	30.11 \pm 5.05	11.83 \pm 1.97	12.39 \pm 1.68	18.12 \pm 9.21	80.111	0.000
FIUD	11.20 \pm 2.29	17.54 \pm 1.97	18.74 \pm 1.85	15.82 \pm 3.90	31.145	0.000
Sum	20.66 \pm 10.47	14.68 \pm 3.50	15.56 \pm 3.69	16.97 \pm 7.09	22.184*	0.000*
F	92.633	33.178	51.228	8.365*	($F=112.365$,	
p	0.000	0.000	0.000	0.006*	$p=0.000$) [#]	

*The F -value and the p -value of the main effect; [#]The F and p -values of the interaction effect.

Detection of the Content of Glutamate in the Hippocampus with HPLC

Hippocampal glutamate concentration was increased after intrauterine fetal distress ($F=280.157, p=0.000$). Two experimental drugs (NMDA receptor antagonists: MK - 801 and CNQX) in the rat hippocampus exerted no apparent effects on the glutamate concentration ($F=0.098, p=0.098$). There was no interaction between fetal distress and glutamate receptor antagonist effect ($F=0.391, p=0.391$) (Table III).

Detection of the Expressions of Tau5, p-PHF1^{Ser396/404}, p-AT8^{Ser199/202}, and p-12E8^{Ser262} Proteins by IHC-SP

Tau protein positive staining was conducted in the hippocampus of the cytoplasm, showing a yellowish brown granule (Figure 1). Protein expressions of p-PHF1^{Ser396/404}, p-AT8^{Ser199/202} and p-12E8^{Ser262} in the rat hippocampus are shown in Figure 2-4. Fetal distress-induced ischemic hypoxia and glutamate receptor antagonists did not significantly affect the expression of total tau protein in the hippocampus of the test rats: Tau 5 protein-IR positive cells (Glutamate receptor antagonist: $F=0.000, p=1.000$), and absorbance of Tau 5 protein-IR positive cells ($F=1.396, p=0.244$) (FIUD: $F=1.600, p=0.213$) (GluR antagonist: $F=0.003, p=0.996$). There were no adverse effects of ischemia and hypoxia and GluR antagonists induced by intrauterine distress (Tau 5

protein-IR positive cells: $F=0.033, p=0.967$) (Tau 5 protein-IR positive cell absorbance: $F=0.029, p=0.970$) (Tables IV and V).

Fetal intrauterine distress-induced hypoxia and hypoxia stress could significantly increase the expression of phosphorylated protein: IR positive cells (p-PHF1^{Ser396/404}: $F=401.364, p=0.000$) (Table VI-VII) (p-AT8^{Ser199/202}: $F=4.186, p=0.047$) (Table VIII-IX) (p-12E8^{Ser262}: $F=319.378, p=0.000$) (Table X-XI), and the absorbance value of IR positive cells (p-PHF1^{Ser396/404}: $F=214.581, p=0.000$) (p-AT8^{Ser199/202}: $F=339.750, p=0.000$) (p-12E8^{Ser262}: $F=199.612, p=0.000$). The glutamate receptor antagonists could reduce the expression of phosphorylated Tau protein: the IR positive cells (p-PHF1^{Ser396/404}: $F=301.431, p=0.000$) (p-AT8^{Ser199/202}: $F=18.556, p=0.000$) (p-12E8^{Ser262}: $F=135.178, p=0.000$), and the absorbance IR value of positive cells (p-PHF1^{Ser396/404}: $F=338.945, p=0.000$) (p-AT8^{Ser199/202}: $F=272.450, p=0.000$) (p-12E8^{Ser262}: $F=206.542, p=0.000$). These two factors interacted with each other: the IR positive cells (p-PHF1^{Ser396/404}: $F=36.743, p=0.000$) (p-AT8^{Ser199/202}: $F=12.463, p=0.000$) (p-12E8^{Ser262}: $F=48.094, p=0.000$), and the absorbance value of IR positive cells (p-PHF1^{Ser396/404}: $F=17.658, p=0.000$) (p-AT8^{Ser199/202}: $F=37.745, p=0.000$) (p-12E8^{Ser262}: $F=18.514, p=0.000$). Glutamate receptor antagonists postponed the hippocampus tau protein phosphorylation triggered by strong fetal intrauterine distress-induced ischemic hypoxia stress.

Table III. The content of glutamate in hippocampus ($\mu\text{mol/gprot}$) ($\bar{x} \pm s, n=8$).

Groups	Saline	MK-801	CNOX	Sum	F	p
Blank	49.30±9.70	52.86±10.72	52.17±10.78	51.44±10.08	0.261	0.772
FIUD	169.534±32.04	158.66±28.98	163.41±32.46	163.87±30.16	0.245	0.786
Sum	109.41±66.15	105.76±58.56	107.79±62.01	107.66±61.00	0.098*	0.906*
F	103.119	93.688	84.542	280.157*	(F=0.391,	
p	0.000	0.001	0.000	0.000*	p=0.678)#	

*The F-value and the p-value of the main effect; #The F and p-values of the interaction effect.

Table IV. The detection of Tau5 protein expression by IHC-SP (Tau5-IR positive cells) ($\bar{x} \pm s, n=8$).

Groups	Saline	MK-801	CNOX	Sum	F	p
Blank	184.87±35.01	187.12±36.39	187.87±33.89	186.61±33.59	0.015	0.984
FIUD	184.87±35.01	187.12±36.39	187.87±33.89	186.61±33.59	0.015	0.984
Sum	192.68±36.75	192.49±35.28	192.62±31.03	192.59±33.69	0.000*	1.000*
F	0.708	0.354	0.358	1.396*	(F=0.033,	
p	0.404	0.561	0.559	0.244*	p=0.967)#	

*The F-value and the p-value of the main effect; #The F and p-values of the interaction effect.

Table V. The detection of Tau5 protein expression by IHC-SP (the absorbance value of IR positive cells) ($\bar{x} \pm s, n=8$).

Groups	Saline	MK-801	CNOX	Sum	F	p
Blank	0.6377±0.1132	0.6398±0.1264	0.6465±0.1093	0.6413±0.1114	0.011	0.988
FIUD	0.6895±0.0981	0.6802±0.1057	0.6786±0.1249	0.6828±0.1054	0.022	0.978
Sum	0.6636±0.1058	0.6802±0.1057	0.6625±0.1146	0.6620±0.1092	0.003*	0.996*
F	0.954	0.480	0.298	1.600*	(F=0.029,	
p	0.345	0.499	0.593	0.213*	p=0.970)#	

*The F-value and the p-value of the main effect; #The F and p-values of the interaction effect.

Table VI. The detection of p-PHF1^{Ser396/404} protein expression by IHC-SP (PHF1-IR positive cells) ($\bar{x} \pm s, n=8$).

Groups	Saline	MK-801	CNOX	Sum	F	p
Blank	36.62±3.06	15.62±2.06	14.87±2.02	22.37±10.55	205.491	0.000
FIUD	77.37±6.66	33.37±5.47	32.74±4.70	47.82±22.01	162.388	0.000
Sum	56.99±21.62	24.49±9.99	23.80±9.86	35.09±21.37	301.431*	0.000*
F	246.171	73.590	38.727	401.364*	(F=36.743,	
p	0.345	0.499	0.593	0.213*	p=0.000)#	

*The F-value and the p-value of the main effect; #The F and p-values of the interaction effect.

Table VII. The detection of p-PHF1^{Ser396/404} protein expression by IHC-SP (the absorbance value of PHF1-IR positive cells) ($\bar{x} \pm s, n=8$).

Groups	Saline	MK-801	CNOX	Sum	F	p
Blank	0.1153±0.0097	0.0649±0.0047	0.0657±0.0055	0.0819±0.0249	133.338	0.000
FIUD	0.1693±0.0134	0.0887±0.0059	0.0908±0.0051	0.1163±0.0392	205.690	0.000
Sum	0.1423±0.0301	0.0768±0.0133	0.0782±0.0139	0.0991±0.0368	338.945*	0.000*
F	83.626	77.656	87.427	214.581*	(F=17.658,	
p	0.000	0.000	0.000	0.000*	p=0.000)#	

*The F-value and the p-value of the main effect; #The F and p-values of the interaction effect.

Table VIII. The detection of p-AT8^{Ser199/202} protein expression by IHC-SP (AT8-IR positive cells) ($\bar{x} \pm s, n=8$).

Groups	Saline	MK-801	CNOX	Sum	F	p
Blank	42.87±8.47	21.87±4.11	20.89±4.08	52.68±31.59	35.102	0.000
FIUD	111.37±11.15	61.87±6.87	57.24±4.45	76.82±26.15	112.670	0.000
Sum	77.12±36.64	41.87±21.36	39.05±19.22	52.68±31.59	18.556*	0.000*
F	191.136	199.221	289.013	4.186*	(F=12.463,	
p	0.000	0.000	0.000	0.047*	p=0.000)#	

*The F-value and the p-value of the main effect; #The F and p-values of the interaction effect.

Table IX. The detection of p-AT8^{Ser199/202} protein expression by IHC-SP (the absorbance value of AT8-IR positive cells) ($\bar{x} \pm s, n=8$).

Groups	Saline	MK-801	CNOX	Sum	F	p
Blank	42.87±8.47	21.87±4.11	20.89±4.08	52.68±31.59	35.102	0.000
FIUD	111.37±11.15	61.87±6.87	57.24±4.45	76.82±26.15	112.670	0.000
Sum	77.12±36.64	41.87±21.36	39.05±19.22	52.68±31.59	18.556*	0.000*
F	191.136	199.221	289.013	4.186*	(F=12.463,	
p	0.000	0.000	0.000	0.047*	p=0.000)#	

*The F-value and the p-value of the main effect; #The F and p-values of the interaction effect.

Table X. The detection of p-12E8^{Ser262} protein expression by IHC-SP (p-12E8Ser262-IR positive cells) ($\bar{x} \pm s$, $n=8$).

Groups	Saline	MK-801	CNOX	Sum	F	p
Blank	24.49±3.24	16.37±1.59	17.12±2.94	19.32±4.54	22.173	0.000
FIUD	59.12±5.37	29.74±4.02	27.74±4.36	38.87±15.29	115.222	0.000
Sum	41.12±18.37	23.05±7.50	22.43±6.55	29.09±14.90	135.178*	0.000*
F	242.483	76.253	32.523	319.378*	($F=48.094$,	
p	0.000	0.000	0.000	0.000*	$p=0.000$)#	

*The F-value and the p-value of the main effect; #The F and p-values of the interaction effect.

Table X. The detection of p-12E8^{Ser262} protein expression by IHC-SP (the absorbance value of 12E8-IR positive cells) ($\bar{x} \pm s$, $n=8$).

Groups	Saline	MK-801	CNOX	Sum	F	p
Blank	0.0881±0.0076	0.0460±0.0041	0.0488±0.0051	0.0610±0.0203	128.009	0.000
FIUD	0.1491±0.0134	0.0747±0.0081	0.0731±0.0128	0.0990±0.0378	108.665	0.000
Sum	0.1186±0.0331	0.0604±0.0160	0.0610±0.0157	0.0800±0.0356	206.542*	0.000*
F	11.402	77.367	24.295	199.612*	($F=18.514$,	
p	0.005	0.000	0.000	0.000*	$p=0.000$)#	

*The F-value and the p-value of the main effect; #The F and p-values of the interaction effect.

Discussion

Tau protein is a highly asymmetric phosphoprotein⁸⁻¹¹. It can maintain smooth neuron axons, and keep the proper distance between tubes and normal axonal transport (axonal transport)¹²⁻¹⁵. The super phosphorylation of Tau protein can significantly weaken its ability to stabilize microtubules, resulting in microtubule assembly disorder, causing neurotransmitter transport and release of obstacles, eventually leading to the dysfunction and impairment of learning and memory¹⁶⁻²². Fetal distress (fetal intrauterine distress)-induced strong ischemia hypoxia stress in most children will result in learning dysmnesia^{23,24}, which may be related to glutamate system (glutamic acid system). Besides, this stress may be closely related to dysfunction²⁵, because it can cause the oxidative stress reaction of many central neurons (oxidative stress reaction)²⁶⁻³¹, resulting in the long range enhancement of the hair (long-term potentiation)³² and nerve dysfunction. Glutamic acid is related to learning, memory and other brain function³³⁻⁴⁰. For example, the stimulation of glutamate can lead to cell membrane depolarization and the overload of neurons within the calcium, and activate the corresponding neural circuits (phosphoinositide loop) and ultrastructure of neurons of subjects, thus resulting in neuron apoptosis and

even death. Therefore, the increase in the strong stress concentration of glutamate in the hippocampus triggered by fetal intrauterine distress-induced ischemic hypoxia stress results in Tau protein phosphorylation, which in turn, causes learning and memory dysfunction. Furthermore, glutamate receptor blockers are able to stop this process, and they have become the focus of many researchers.

The results revealed that the Tau protein phosphorylation level was associated with cognitive ability. Tau protein structure features a lot of amino acid residues repeat area, namely the Pro-Gly-Gly-Gly series “repeat” constitutes a combination of Tau protein zone, which stabilizes the microtubule assembly, keeps an appropriate distance between tubes, and regulates neuron axon transport capacity in the end. Under physiological conditions, Tau protein phosphorylation can reduce the transportation efficiency of neurons axon, resulting in synaptic degeneration of neurons, neuronal apoptosis, and cognitive impairment. The results of the experiments are consistent with those of the related research; strong fetal intrauterine distress-induced ischemic hypoxia stress can lead to a significant rise in concentration of glutamic acid in the hippocampus, which in turn induces Tau protein in the hippocampus neuron change excessive phosphorylation.

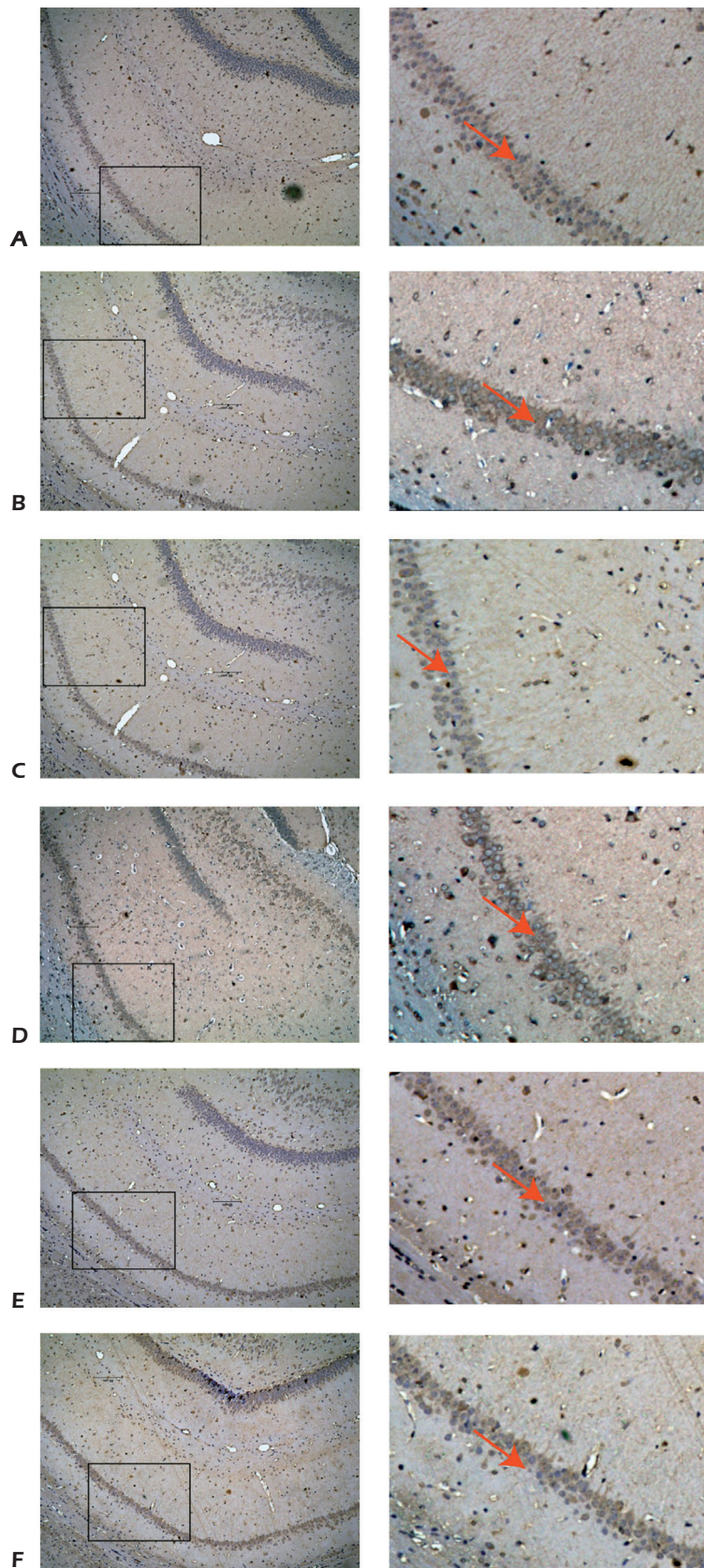
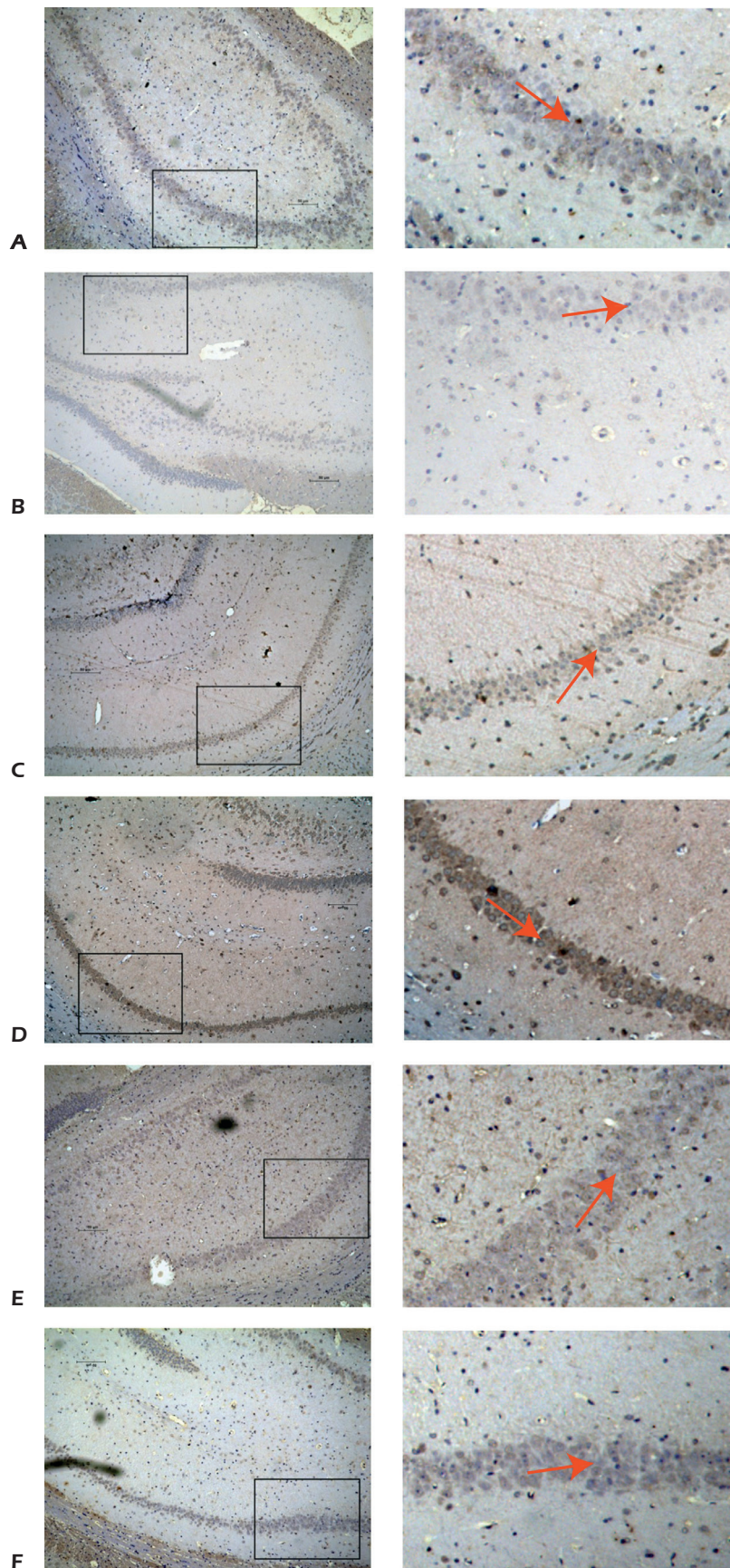


Figure 1. The prediction probability ROC curve of test sample Figure 1. Tau protein expression in rat hippocampus by IHC-SP (100 ×). **A**, Group S (2 mL saline injected *via* tail vein). **B**, Group M (2 mL MK-801 is injected *via* tail vein, 5 mg/kg). **C**, Group D (2 mL AMPAR antagonists are injected *via* tail vein, 5 mg/kg). **D**, Group SE (2 mL saline is injected *via* tail vein +FIUD in that the uterine arteries of pregnant rat will be blocked moderately for 10 min). **E**, Group ME (2 mL MK-801 antagonists are injected *via* tail vein, 5 mg/kg +FIUD in that the uterine arteries of pregnant rat will be blocked moderately for 10 min). **F**, Group DE (2 mL AMPAR antagonists are injected *via* tail vein , 5 mg/kg + in that the uterine arteries of pregnant rat will be blocked moderately for 10 min).

Figure 2. p-PHF1^{Ser396/404} protein expression in rat hippocampus by IHC-SP (100 ×). **A**, Group S (2 mL saline is injected *via* tail vein). **B**, Group M (2 mL MK-801 injected *via* tail vein, 5 mg/kg). **C**, Group D (2 mL AMPAR antagonists are injected *via* tail vein, 5 mg/kg). **D**, Group SE (2 mL saline is injected *via* tail vein +FIUD in that the uterine arteries of pregnant rat will be blocked moderately for 10 min). **E**, Group ME (2 mL MK-801 antagonists are injected *via* tail vein, 5 mg/kg +FIUD in that the uterine arteries of pregnant rat will be blocked moderately for 10 min). **F**, Group DE (2 mL AMPAR antagonists are injected *via* tail vein, 5 mg/kg + in that the uterine arteries of pregnant rat will be blocked moderately for 10 min).



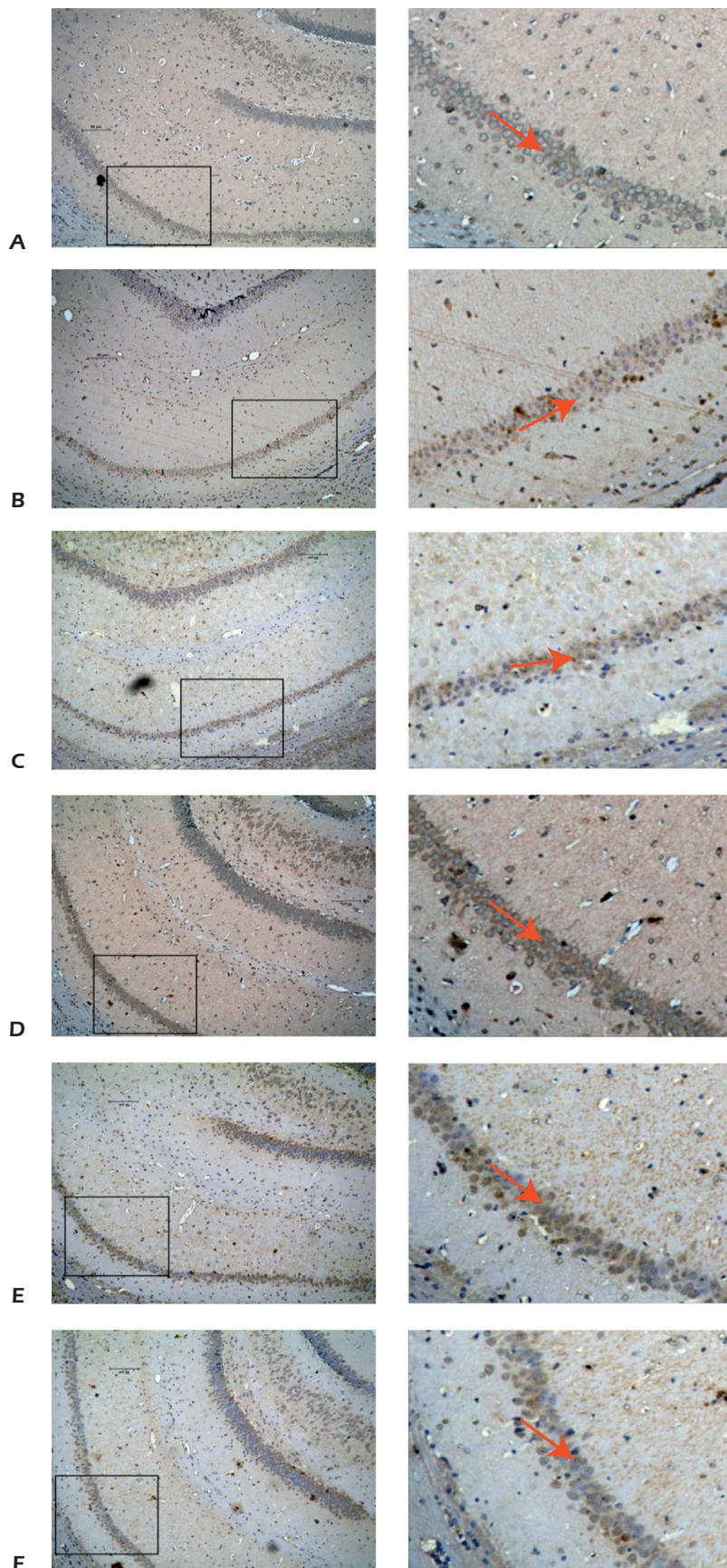
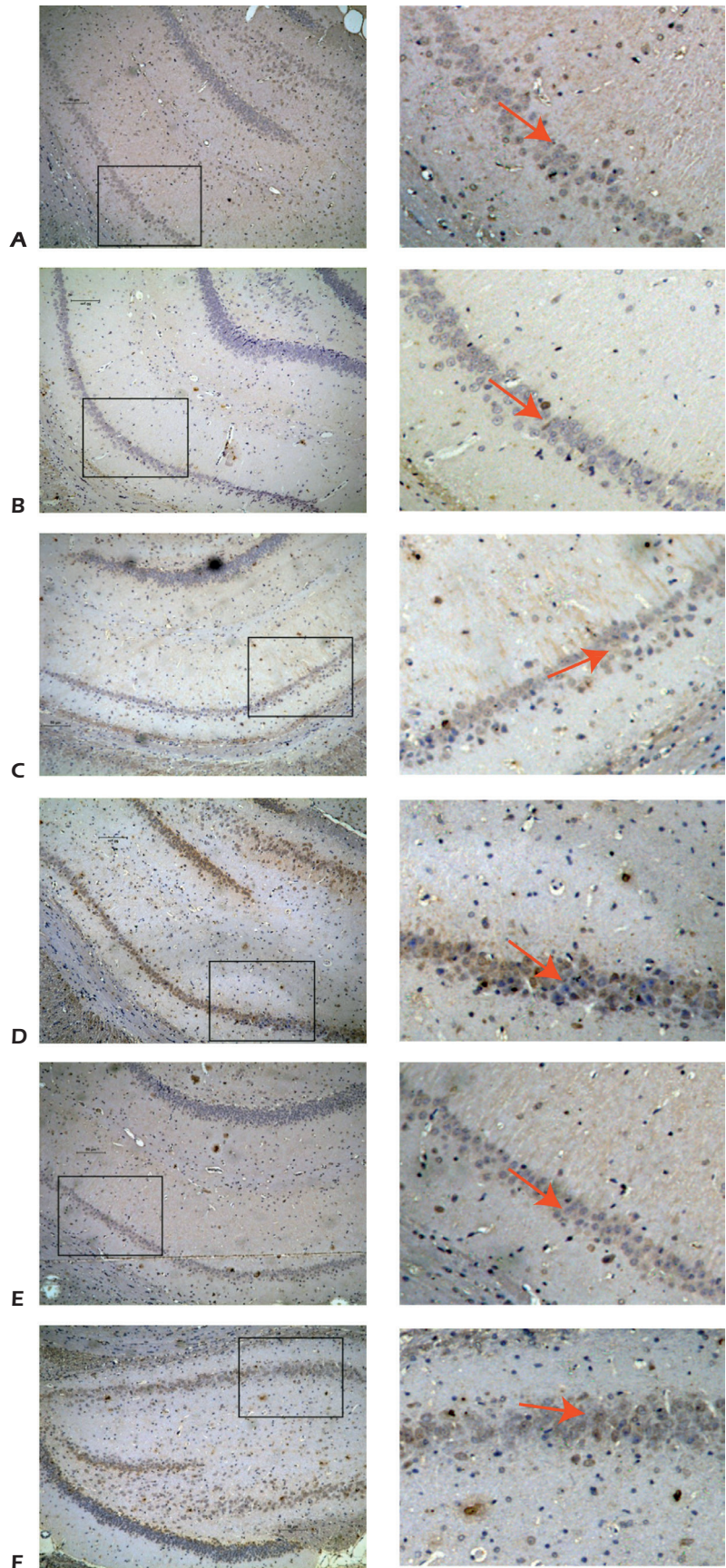


Figure 3. p-AT8^{Ser199/202} protein expression in rat hippocampus by IHC-SP (100 ×). **A**, Group S (2 mL saline is injected *via* tail vein), **B**, Group M (2 ml MK-801 is injected *via* tail vein, 5 mg/kg), **C**, Group D (2 mL AMPAR antagonists are injected *via* tail vein, 5 mg/kg). **D**, Group SE (2 mL saline is injected *via* tail vein +FIUD in that the uterine arteries of pregnant rat will be blocked moderately for 10 min), **E**, Group ME (2 mL MK-801 antagonists are injected *via* tail vein, 5 mg/kg +FIUD in that the uterine arteries of pregnant rat will be blocked moderately for 10 min), **F**, Group DE (2 mL AMPAR antagonists are injected *via* tail vein , 5 mg/kg + in that the uterine arteries of pregnant rat will be blocked moderately for 10 min).

Figure 4. p-12E8^{Ser262} protein expression in rat hippocampus by IHC-SP (100×). **A**, Group S (2 mL saline injected *via* tail vein). **B**, Group M (2 mL MK-801 is injected *via* tail vein, 5 mg/kg). **C**, Group D (2 mL AMPAR antagonists re injected *via* tail vein, 5 mg/kg). **D**, Group SE (2 mL saline is injected *via* tail vein +FIUD in that the uterine arteries of pregnant rat will be blocked moderately for 10 min). **E**, Group ME (2 mL MK-801 antagonists are injected *via* tail vein, 5 mg/kg +FIUD in that the uterine arteries of pregnant rat will be blocked moderately for 10 min). **F**, Group DE (2 mL AMPAR antagonists are injected *via* tail vein, 5 mg/kg + in that the uterine arteries of pregnant rat will be blocked moderately for 10 min).



In addition, the results manifested that, among many Tau protein phosphorylation sites, pSer^{199/202} loci of phosphorylation are closely associated with fetal intrauterine distress stress. The experimental results indicated that as Ser^{199/202} site is located at the junction of the Tau protein in the area, Tau protein microtubules in combination with the degree of phosphorylation activity were selected. Glutamate is the most important excitatory neurotransmitter, which has biphasic effect on learning and memory; it has an appropriate concentration of glutamic acid can properly excite Glu receptor within the appropriate neurons. This will promote learning, memory and other brain functions normally. However, if there are excessive generated and released glutamates, glutamate receptors can be over-excited, resulting in cognitive impairment. The results suggest that fetal intrauterine distress-induced ischemic hypoxia stress can lead to excitatory toxicity, and glutamate receptor antagonists can alleviate glutamate concentration caused by the excessive rise of Tau protein phosphorylation. This improves the strong stress, thus leading to the dysfunction of learning and memory, which is consistent with previous experimental results. Then, the mechanism is needed of further investigations.

Conclusions

Fetal intrauterine distress-induced ischemic hypoxia stress can cause excessive synthesis and release of glutamates in the hippocampus, which in turn induce excitatory toxic reaction and excessive phosphorylation reaction of Tau protein in the hippocampus. This results impaired brain function such as learning and memory. Glutamate receptor antagonists (including NMDA receptor antagonist and AMPA receptor antagonist) can alleviate neuronal excitability toxicity reaction induced by a high concentration of glutamic acids, slow down the excessive Tau protein phosphorylation in the hippocampus, and eventually improve cognitive impairment caused by the fetal intrauterine distress-induced ischemia hypoxia stress.

Conflict of Interest

The authors declared no conflict of interest.

References

- ZHOU B, WANG CH, DING RB, CHEN JG, CHE YH, DENG YX. The relationship between the internal oxidation-reduction system and fetal distress on pregnant patients with intrahepatic cholestasis. *Eur Rev Med Pharmacol Sci* 2015; 19: 3817-3821.
- CHEN Q, ZHANG F, WANG Y, LIU Z, SUN A, ZEN K, ZHANG CY, ZHANG Q. The transcription factor c-Myc suppresses MiR-23b and MiR-27b transcription during fetal distress and increases the sensitivity of neurons to hypoxia-induced apoptosis. *PLoS One* 2015; 10: e120217.
- KIM YM, PARK JY, SUNG JH, CHOI SJ, OH SY, ROH CR, KIM JH. Predicting factors for success of vaginal delivery in preterm induction with prostaglandin E2. *Obstet Gynecol Sci* 2017; 60: 163-169.
- WARMERDAM GJ, VULLINGS R, VAN LAAR JO, VAN DER HOUT-VAN DJM, BERGMANS JW, SCHMITT L, OEI SG. Selective heart rate variability analysis to account for uterine activity during labor and improve classification of fetal distress. *Conf Proc IEEE Eng Med Biol Soc* 2016; 2016: 2950-2953.
- JULIAN GS, OLIVEIRA RW, FAVARO VM, OLIVEIRA MG, PERRY JC, TUFIK S, CHAGAS JR. Chronic intermittent hypoxia increases encoding pigment epithelium-derived factor gene expression, although not that of the protein itself, in the temporal cortex of rats. *J Bras Pneumol* 2015; 41: 39-47.
- SINGH M, KAMAL YT, KHAN MA, PARVEEN R, ANSARI SH, AHMAD S. Matrix solid-phase dispersion extraction and quantification of alpinetin in amomum seed using validated HPLC and HPTLC methods. *Indian J Pharm Sci* 2015; 77: 49-54.
- HU P, WANG G, SHEN M, ZHANG P, ZHANG J, DU J, LIU Q. Intratumoral polymorphonuclear granulocyte is associated with poor prognosis in squamous esophageal cancer by promoting epithelial-mesenchymal transition. *Future Oncol* 2015; 11: 771-783.
- ZHI XL, LI CY, XUE M, HU Y, JI Y. Changes in cognitive function due to combined propofol and remifentanyl treatment are associated with phosphorylation of Tau in the hippocampus, abnormal total water and calcium contents of the brain, and elevated serum S100 β levels. *Eur Rev Med Pharmacol Sci* 2016; 20: 2156-2162.
- LUO DJ, FENG Q, WANG ZH, SUN DS, WANG Q, WANG JZ, LIU GP. Knockdown of phosphotyrosyl phosphatase activator induces apoptosis via mitochondrial pathway and the attenuation by simultaneous tau hyperphosphorylation. *J Neurochem* 2014; 130: 816-825.
- TAN YJ, SUI D, WANG WH, KUO MH, REID GE, BRUENING ML. Phosphopeptide enrichment with TiO₂-modified membranes and investigation of tau protein phosphorylation. *Anal Chem* 2013; 85: 5699-5706.
- GUO T, NOBLE W, HANGER DP. Roles of tau protein in health and disease. *Acta Neuropathol* 2017; 133: 665-704.
- ZEMPEL H, MANDELKOW E. Lost after translation: mis-sorting of tau protein and consequences for Alzheimer disease. *Trends Neurosci* 2014; 37: 721-732.

- 13) KUZNETSOV IA, KUZNETSOV AV. What tau distribution maximizes fast axonal transport toward the axonal synapse? *Math Biosci* 2014; 253: 19-24.
- 14) ONISHI T, MATSUMOTO Y, HATTORI M, OBAYASHI Y, NAKAMURA K, YANO T, Horiguchi T, IWASHITA H. Early-onset cognitive deficits and axonal transport dysfunction in P301S mutant tau transgenic mice. *Neurosci Res* 2014; 80: 76-85.
- 15) RAMSER EM, GAN KJ, DECKER H, FAN EY, SUZUKI MM, FERREIRA ST, SILVERMAN MA. Amyloid-beta oligomers induce tau-independent disruption of BDNF axonal transport via calcineurin activation in cultured hippocampal neurons. *Mol Biol Cell* 2013; 24: 2494-2505.
- 16) KANNO T, TSUCHIYA A, NISHIZAKI T. Hyperphosphorylation of Tau at Ser396 occurs in the much earlier stage than appearance of learning and memory disorders in 5XFAD mice. *Behav Brain Res* 2014; 274: 302-306.
- 17) JIN G, WANG LH, JI XF, CHI TY, QI Y, JIAO Q, XU Q, ZHOU XY, ZHANG R, ZOU LB. Xanthoceraside rescues learning and memory deficits through attenuating beta-amyloid deposition and tau hyperphosphorylation in APP mice. *Neurosci Lett* 2014; 573: 58-63.
- 18) BRIONES TL, DARWISH H. Decrease in age-related tau hyperphosphorylation and cognitive improvement following vitamin D supplementation are associated with modulation of brain energy metabolism and redox state. *Neuroscience* 2014; 262: 143-155.
- 19) FARR SA, RIPLEY JL, SULTANA R, ZHANG Z, NIEHOFF ML, PLATT TL, MURPHY MP, MORLEY JE, KUMAR V, BUTTERFIELD DA. Antisense oligonucleotide against GSK-3beta in brain of SAMP8 mice improves learning and memory and decreases oxidative stress: involvement of transcription factor Nrf2 and implications for Alzheimer disease. *Free Radic Biol Med* 2014; 67: 387-395.
- 20) XIONG H, ZHENG C, WANG J, SONG J, ZHAO G, SHEN H, DENG Y. The neuroprotection of liraglutide on Alzheimer-like learning and memory impairment by modulating the hyperphosphorylation of tau and neurofilament proteins and insulin signaling pathways in mice. *J Alzheimers Dis* 2013; 37: 623-635.
- 21) BEHARRY C, ALANIZ ME, ALONSO AC. Expression of Alzheimer-like pathological human tau induces a behavioral motor and olfactory learning deficit in *Drosophila melanogaster*. *J Alzheimers Dis* 2013; 37: 539-550.
- 22) NAKAJIMA A, AOYAMA Y, NGUYEN TT, SHIN EJ, KIM HC, YAMADA S, NAKAI T, NAGAI T, YOKOSUKA A, MIMAKI Y, OHIZUMI Y, YAMADA K. Nobiletin, a citrus flavonoid, ameliorates cognitive impairment, oxidative burden, and hyperphosphorylation of tau in senescence-accelerated mouse. *Behav Brain Res* 2013; 250: 351-360.
- 23) PATRIANAKOS-HOOBLER AI, MARKS JD, MSALL ME, HUO D, SCHREIBER MD. Safety and efficacy of inhaled nitric oxide treatment for premature infants with respiratory distress syndrome: follow-up evaluation at early school age. *Acta Paediatr* 2011; 100: 524-528.
- 24) JADAS V, BRASSEUR-DAUDRUY M, CHOLLAT C, PELLERIN L, DEVAUX AM, MARRSET S. [the contribution of the clinical examination, electroencephalogram, and brain MRI in assessing the prognosis in term newborns with neonatal encephalopathy. A cohort of 30 newborns before the introduction of treatment with hypothermia]. *Arch Pediatr* 2014; 21: 125-133.
- 25) ZLOTNIK A, TSEHIS S, GRUENBAUM BF, OHAYON S, GRUENBAUM SE, BOYKO M, SHEINER E, BROTFAIN E, SHAPIRA Y, TEICHBERG VI. Relationship between glutamate, GOT and GPT levels in maternal and fetal blood: a potential mechanism for fetal neuroprotection. *Early Hum Dev* 2012; 88: 773-778.
- 26) DE BUNDEL D, SCHALLIER A, LOYENS E, FERNANDO R, MIYASHITA H, VAN LIEFFERINGE J, VERMOESEN K, BANNAI S, SATO H, MICHOTTE Y, SMOLDERS I, MASSIE A. Loss of system x(c)- does not induce oxidative stress but decreases extracellular glutamate in hippocampus and influences spatial working memory and limbic seizure susceptibility. *J Neurosci* 2011; 31: 5792-5803.
- 27) OSBORNE NN, JI D, MAJID AS, DEL SP, SPARATORE A. Glutamate oxidative injury to RGC-5 cells in culture is necrostatin sensitive and blunted by a hydrogen sulfide (H₂S)-releasing derivative of aspirin (ACS14). *Neurochem Int* 2012; 60: 365-378.
- 28) ALBRECHT P, HENKE N, TIEN ML, ISSBERNER A, BOUCHACHIA I, MAHER P, LEWERENZ J, METHNER A. Extracellular cyclic GMP and its derivatives GMP and guanosine protect from oxidative glutamate toxicity. *Neurochem Int* 2013; 62: 610-619.
- 29) BETZEN C, WHITE R, ZEHENDNER CM, PIETROWSKI E, BENDER B, LUHMANN HJ, KUHLMANN CR. Oxidative stress upregulates the NMDA receptor on cerebrovascular endothelium. *Free Radic Biol Med* 2009; 47: 1212-1220.
- 30) DAS A, BELAGODU A, REITER RJ, RAY SK, BANIK NL. Cytoprotective effects of melatonin on C6 astroglial cells exposed to glutamate excitotoxicity and oxidative stress. *J Pineal Res* 2008; 45: 117-124.
- 31) KAWAKAMI Z, KANNO H, IKARASHI Y, KASE Y. Yokukansan, a kampo medicine, protects against glutamate cytotoxicity due to oxidative stress in PC12 cells. *J Ethnopharmacol* 2011; 134: 74-81.
- 32) GUERREIRO S, PONCEAU A, TOULORGE D, MARTIN E, ALVAREZ-FISCHER D, HIRSCH EC, MICHEL PP. Protection of mid-brain dopaminergic neurons by the end-product of purine metabolism uric acid: potentiation by low-level depolarization. *J Neurochem* 2009; 109: 1118-1128.
- 33) ORTIZ JB, TAYLOR SB, HOFFMAN AN, CAMPBELL AN, LUCAS LR, CONRAD CD. Sex-specific impairment and recovery of spatial learning following the end of chronic unpredictable restraint stress: potential relevance of limbic GAD. *Behav Brain Res* 2015; 282: 176-184.
- 34) TANAKA-HAYASHI A, HAYASHI S, INOUE R, ITO T, KONNO K, YOSHIDA T, WATANABE M, YOSHIMURA T, MORI H. Is D-aspartate produced by glutamic-oxaloacetic transaminase-1 like 1 (Got111): a putative aspartate racemase? *Amino Acids* 2015; 47: 79-86.
- 35) SHIN MK, KIM HG, BAEK SH, JUNG WR, PARK DI, PARK JS, JO DG, KIM KL. Neuropep-1 ameliorates learning and memory deficits in an Alzheimer's disease mouse model, increases brain-derived neurotrophic factor expression in the brain, and causes reduction of amyloid beta plaques. *Neurobiol Aging* 2014; 35: 990-1001.
- 36) YANG EJ, PARK GH, SONG KS. Neuroprotective effects of liquiritigenin isolated from licorice roots on glutamate-induced apoptosis in hippocampal neuronal cells. *Neurotoxicology* 2013; 39: 114-123.

- 37) GONZALEZ P, MACHADO I, VILCAES A, CARUSO C, ROTH GA, SCHIOTH H, LASAGA M, SCIMONELLI T. Molecular mechanisms involved in interleukin 1-beta (IL-1beta)-induced memory impairment. Modulation by alpha-melanocyte-stimulating hormone (alpha-MSH). *Brain Behav Immun* 2013; 34: 141-150.
- 38) FRISCH C, MALTER MP, ELGER CE, HELMSTAEDTER C. Neuropsychological course of voltage-gated potassium channel and glutamic acid decarboxylase antibody related limbic encephalitis. *Eur J Neurol* 2013; 20: 1297-1304.
- 39) KLUSA V, MUCENIECE R, ISAJEV S, ISAJEVA D, BEITNERE U, MANDRIKA I, PUPURE J, RUMAKS J, JANSONE B, KALVINSH I, VINTERS HV. Mildronate enhances learning/memory and changes hippocampal protein expression in trained rats. *Pharmacol Biochem Behav* 2013; 106: 68-76.
- 40) GUZMAN-RAMOS K, MORENO-CASTILLA P, CASTRO-CRUZ M, MCGAUGH JL, MARTINEZ-CORIA H, LA FERLA FM, BERMUDEZ-RATTONI F. Restoration of dopamine release deficits during object recognition memory acquisition attenuates cognitive impairment in a triple transgenic mice model of Alzheimer's disease. *Learn Mem* 2012; 19: 453-460.